

Dynamical behaviors of a multifunctional neural circuit

Xiao-Hong Gao(高晓红), Kai-Long Zhu(朱凯龙), and Fei-Fei Yang(杨飞飞)
Citatio: Chin. Phys. B, 2025, 34 (**9**): 090503. DOI: 10.1088/1674-1056/ae001b
http://cpb.iphy.ac.cn; http://iopscience.iop.org/cpb

What follows is a list of articles you may be interested in

A novel non-autonomous hyperchaotic map based on discrete memristor parallel connection

Weiping Wu(吴伟平), Mengjiao Wang(王梦蛟), and Qigui Yang(杨启贵)
Chin. Phys. B, 2025, 34 (**5**): 050503. DOI: 10.1088/1674-1056/adb8bc

Dynamical analysis, control, boundedness, and prediction for a fractional-order financial risk system

Kehao Yang(杨轲皓), Song Zheng(郑松), Tianhu Yu(余天虎), Aceng Sambas, Muhamad Deni Johansyah, Hassan Saberi-Nik, and Mohamad Afendee Mohamed
Chin. Phys. B, 2024, 33 (**11**): 110501. DOI: 10.1088/1674-1056/ad7afb

Memristors-coupled neuron models with multiple firing patterns and homogeneous and heterogeneous multistability

Xuan Wang(王暄), Santo Banerjee, Yinghong Cao(曹颖鸿), and Jun Mou(牟俊)
Chin. Phys. B, 2024, 33 (**10**): 100501. DOI: 10.1088/1674-1056/ad6256

Effects of asymmetric coupling and boundary on the dynamic behaviors of a random nearest neighbor coupled system

Ling Xu(徐玲) and Lei Jiang(姜磊)
Chin. Phys. B, 2024, 33 (**6**): 060503. DOI: 10.1088/1674-1056/ad3b86

A multiple-relaxation-time lattice Boltzmann method for high-speed compressible flows

Li Kai (李凯), Zhong Cheng-Wen (钟诚文)
Chin. Phys. B, 2015, 24 (**5**): 050501. DOI: 10.1088/1674-1056/24/5/050501

Dynamical behaviors of a multifunctional neural circuit

Xiao-Hong Gao(高晓红)[1,†], Kai-Long Zhu(朱凯龙)[2], and Fei-Fei Yang(杨飞飞)[2]

[1] *College of New Energy, Longdong University, Qingyang* 745000, *China*

[2] *College of Artificial Intelligence and Computer Science, Xi'an University of Science and Technology, Xi'an* 710054, *China*

(Received 19 July 2025; revised manuscript received 27 August 2025; accepted manuscript online 28 August 2025)

Biological neurons exhibit a double-membrane structure and perform specialized functions. Replicating the double-membrane architecture in artificial neurons to mimic biological neuronal functions is a compelling research challenge. In this study, we propose a multifunctional neural circuit composed of two capacitors, two linear resistors, a phototube cell, a nonlinear resistor, and a memristor. The phototube and charge-controlled memristor serve as sensors for external light and electric field signals, respectively. By applying Kirchhoff's and Helmholtz's laws, we derive the system's nonlinear dynamical equations and energy function. We further investigate the circuit's dynamics using methods from nonlinear dynamics. Our results show that the circuit can exhibit both periodic and chaotic patterns under stimulation by external light and electric fields.

Keywords: multifunctional neural circuit, energy distribution, dynamical behaviors

PACS: 05.45.–a

DOI: 10.1088/1674-1056/ae001b **CSTR:** 32038.14.CPB.ae001b

1. Introduction

Neuron modeling is a key research area in neuroscience that aims to describe neuronal behavior and network dynamics using mathematical and computational approaches. Various modeling methods exist, including conductance-based models, integrate-and-fire models, and rate-based models, each suited for different research objectives and complexity levels. Based on their complexity and intended applications, numerous neuron models have been proposed, including Hodgkin–Huxley (H–H) model,[1] Morris–Lecar (M–L) model,[2] integrate-and-fire (I–F) model,[3] Hindmarsh–Rose (H–R) model,[4] Chay model,[5] Izhikevich model[6], and Chialvo model.[7] These models can accurately simulate the complex dynamical behaviors of biological neurons.

However, it is extremely difficult to explore the collective dynamics of functional neurons and networks through biological experiments. From a physics perspective, constructing neuron models with nonlinear circuits offers a promising research direction. Moreover, neural circuits constructed from functional electronic components can effectively emulate the electrophysiological properties of biological neurons. For instance, Liu *et al.*[8] developed a photocurrent-activated neural circuit that models retinal phototransduction. Xu *et al.*[9] proposed a temperature-sensitive neuron model to characterize biological neurons' thermosensitive properties. Guo *et al.*[10] developed an auditory neuron model by incorporating a piezoelectric ceramic element into a nonlinear circuit to simulate mammalian cochlear function. Furthermore, incorporating two functional elements into a neural circuit enables the realization of multifunctional neuron models. For instance, light-temperature-sensitive neuron models[11–13] have been developed by integrating both a thermistor and a phototube into the circuit design.

Recently, owing to their unique memory properties, memristors have been widely employed in neuron and neural network modeling to emulate synaptic plasticity and biological information processing mechanisms. For example, magnetic flux-controlled memristor neuron models,[14–16] charge-controlled memristive neuron models,[17] dual memristor neuron models,[18,19] memristive membrane neuron models,[20–22] memristive ion channel neuron models,[23–25] local active memristor neuron models,[26–28] memristive neuron networks,[29–31] memristor map neurons,[32–34] and memristive map neuron networks.[35,36]

Although numerous functional neuron models have been developed, most existing designs are functionally limited and structurally simplistic, generally exhibiting single-membrane characteristics that fail to replicate the dual-membrane architecture of biological neurons accurately. Building upon existing research on functional neurons and memristive neural models, this study proposes a novel multifunctional neural circuit with a dual membrane and systematically investigates its dynamical characteristics. The main contributions of this study are summarized as follows:

(i) This paper proposes a bio-inspired double-membrane neuron structure implemented using a linear resistor coupled with two capacitors, faithfully replicating the fundamental architecture of biological neurons.

(ii) A novel sensing mechanism is developed by integrat-

[†]Corresponding author. E-mail: gaoxh0219@126.com

© 2025 Chinese Physical Society and IOP Publishing Ltd. All rights, including for text and data mining, AI training, and similar technologies, are reserved.

ing a phototube with a charge-controlled memristor, enabling simultaneous detection of external optical signals and electric field stimuli.

(iii) The system's Hamilton energy function is analytically derived using Helmholtz's theorem, providing theoretical insights into the circuit's energy dynamics.

The remainder of this paper is organized as follows: Section 2 presents the design of an inductor-free multifunctional neural circuit. Section 3 investigates the dynamical behaviors of the proposed neuron model. Finally, Section 4 provides concluding remarks and discusses potential applications.

2. Model of a multifunctional neural circuit

Figure 1 illustrates our proposed multifunctional nonlinear circuit, designed to replicate the functionality of biological neurons.

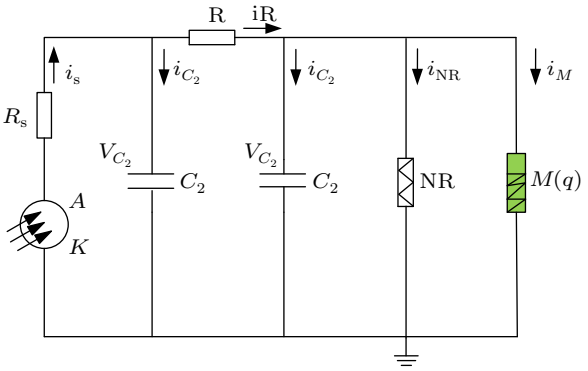


Fig. 1. A functional neural circuit without inductor.

The proposed circuit in Fig. 1 comprises five functional branches, collectively emulating key properties of biological neurons: The optical sensing branch (phototube in series with resistor R) converts external light stimuli into electrical signals. The dual-membrane simulation module (branches 2 and 3) employs resistively-coupled capacitors to replicate biological membrane dynamics. The nonlinear conversion branch (nonlinear resistor NR) models electromagnetic field energy transformation. The electric field detection branch (voltage-controlled memristor $M(q)$) captures external electrical stimuli.

To derive the circuit equations, the current in the fourth branch (nonlinear resistor NR) is approximated as follows:

$$i_{\mathrm{NR}} = -\frac{1}{\rho}\left(V - \frac{V^3}{3V_0^2}\right). \tag{1}$$

Here, ρ denotes the resistance, V the voltage, and V_0 the reverse cutoff voltage. The memristor in the fifth branch (voltage-controlled memristor $M(q)$) is defined by

$$V_M = M(q)i_M = \frac{1}{k_M}\csc q \cdot i_M, \quad \frac{\mathrm{d}q}{\mathrm{d}t} = dq + i_M, \tag{2}$$

where i_M represents the current, V_M the voltage, q the charge, and d and k_M are parameters. The current in the first branch (phototube in series with resistor R) is calculated as

$$i_{\mathrm{s}} = \frac{V_{\mathrm{p}} - V}{R_{\mathrm{s}}}, \tag{3}$$

where i_{s} denotes the current, R_{S} the resistor, and V and V_{p} the voltages. Applying Kirchhoff's law, the circuit equations for the multifunctional neural circuit are given by

$$\begin{cases} C_1\dfrac{\mathrm{d}V_{C_1}}{\mathrm{d}t} = \dfrac{V_{C_2}-V_{C_1}}{R} + \dfrac{1}{\rho}\left(V_{C_1} - \dfrac{V_{C_1}^3}{3V_0}\right) i_{\mathrm{NR}} - k_M \sin(q)V_{C_1}, \\ C_2\dfrac{\mathrm{d}V_{C_2}}{\mathrm{d}t} = \dfrac{V_{C_1}-V_{C_2}}{R} + \dfrac{V_{\mathrm{p}}-V_{C_2}}{R_{\mathrm{S}}}, \\ \dfrac{\mathrm{d}q}{\mathrm{d}t} = dq + k_M \sin(q)V_{C_1}. \end{cases} \tag{4}$$

To facilitate dynamical analysis, we introduce the following dimensionless transformations for the variables and parameters in Eq. (4):

$$\begin{cases} x = \dfrac{V_{C_1}}{V_0},\ y = \dfrac{V_{C_2}}{V_0},\ z = \dfrac{q}{C_1V_0},\ \tau = \dfrac{t}{\rho C_2}, \\ \alpha = \dfrac{C_2}{C_1},\ \beta = \dfrac{R}{\rho},\ \gamma = \dfrac{R}{R_{\mathrm{s}}},\ u_{\mathrm{s}} = \dfrac{V_{\mathrm{p}}R}{R_{\mathrm{s}}V_0}, \\ k = C_1V_0,\ b = k_MR,\ c = RdC_1. \end{cases} \tag{5}$$

Therefore, the dynamical system described by Eq. (4) can be represented in normalized form as

$$\begin{cases} \dfrac{\mathrm{d}x}{\mathrm{d}\tau} = \alpha\left[y - x + \beta\left(x - \dfrac{x^3}{3}\right) - bx\sin(kz)\right], \\ \dfrac{\mathrm{d}y}{\mathrm{d}\tau} = x - (1+\gamma)y + u_{\mathrm{s}}, \\ \dfrac{\mathrm{d}z}{\mathrm{d}\tau} = \alpha(cz + bx\sin(kz)). \end{cases} \tag{6}$$

Since the charge-controlled memristor in the fifth branch can capture the external electric field, the dynamic equations in Eq. (4) can also be expressed as

$$\begin{cases} \dfrac{\mathrm{d}x}{\mathrm{d}\tau} = \alpha\left[y - x + \beta\left(x - \dfrac{x^3}{3}\right) - bx\sin(kz)\right], \\ \dfrac{\mathrm{d}y}{\mathrm{d}\tau} = x - (1+\gamma)y + u_{\mathrm{s}}, \\ \dfrac{\mathrm{d}z}{\mathrm{d}\tau} = \alpha(cz + bx\sin(kz)) + S_{\mathrm{ext}}, \end{cases} \tag{7}$$

where S_{ext} denotes the external electric field. Furthermore, the physical field energies of the multifunctional neural circuit are calculated by

$$W = \frac{CV_{C_1}^2}{2} + \frac{CV_{C_2}^2}{2} + \frac{qV_{C_1}}{2}. \tag{8}$$

As a result, the dimensionless Hamilton energy in Eq. (8) is

$$H = \frac{W}{C_1V_0^2} = \frac{x^2}{2\alpha} + \frac{y^2}{2} + \frac{xz}{2\alpha}. \tag{9}$$

It is known from Helmholtz's theorem that the energy function satisfies

$$\begin{cases} (-\alpha y-\alpha c x)\dfrac{\partial H}{\partial x}+(x+z/2)\dfrac{\partial H}{\partial y}+(\alpha c z+2acx)\dfrac{\partial H}{\partial z}=0, \\ \dfrac{\mathrm{d}H}{\mathrm{d}\tau}=\left\{\alpha\left[2y-x+\beta\left(x-\dfrac{x^3}{3}\right)-bx\sin(kz)-cx\right]\right\} \\ \quad\times\left(\dfrac{x}{\alpha}+\dfrac{z}{2\alpha}\right)+\left[-(1+\gamma)y+u_{\mathrm{s}}-\dfrac{z}{2}\right]y \\ \quad+(\alpha bx\sin(kz)-2acx)\dfrac{z}{2\alpha} \\ \quad=\nabla H^{\mathrm{T}}F_{\mathrm{d}}(x,y,z). \end{cases} \tag{10}$$

3. Dynamical behaviors of a multifunctional neural circuit

Dynamical behaviors of the multifunctional neural circuit are analyzed through nonlinear dynamics methods. First, we investigate how external light signals modulate the system's dynamics. Parameters in Eq. (6) are set as $\beta=2$, $\gamma=0.1$, $\alpha=1$, $b=0.5$, $k=1$, and $c=-0.5$. The light stimulus is modeled as $u_{\mathrm{s}}=A\cos(0.8\tau)$. Using initial conditions ($x=0.01$, $y=0.1$, $z=0.01$), Fig. 2 presents the bifurcation diagram (BD) and largest Lyapunov exponent (LLE) versus varying amplitude A.

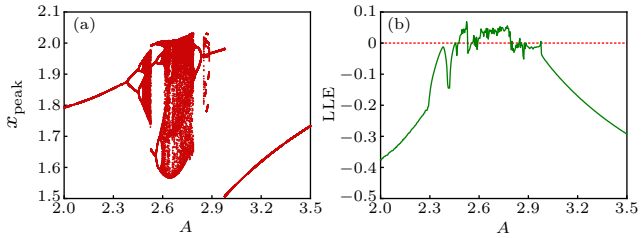


Fig. 2. BD and LLE for different A. For (a) BD under $A\in[2,3.5]$; (b) LLE under $A\in[2,3.5]$.

Figure 2 demonstrates that modulating the amplitude parameter A can induce both periodic and chaotic patterns in the multifunctional neural circuit. In nonlinear dynamical systems, these distinct oscillation modes exhibit characteristic evolutionary trajectories and energy distribution profiles. Furthermore, Fig. 3 compares the temporal evolution of the state variable x and Hamiltonian energy H for different values of A, highlighting their amplitude-dependent behaviors.

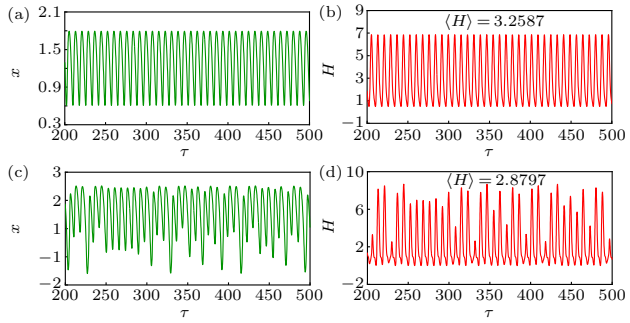


Fig. 3. The x and H by changing A. For (a) and (b) $A=2$ (periodic); (c) and (d) $A=2.75$ (chaotic).

Figure 3 reveals distinct energy distribution patterns between different oscillation modes: periodic states exhibit higher mean energy values $\langle H\rangle$, while chaotic regimes show significantly lower $\langle H\rangle$. Furthermore, for the specific case of $u_{\mathrm{s}}=2.75\cos(0.8\tau)$, we examine the frequency-dependent dynamics through BD and LLE. Figure 4 presents the corresponding BD and LLE as functions of driving frequency f.

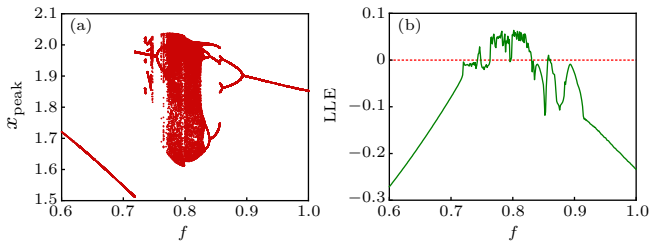


Fig. 4. BD and LLE by changing f. For (a) BD under $f\in[0.6,1]$; (b) LLE under $f\in[0.6,1]$.

Consistent with the findings in Fig. 2, both periodic and chaotic patterns emerge in the multifunctional neural circuit when varying the frequency parameter f. Figure 5 further illustrates this frequency-dependent behavior by comparing the temporal evolution of state variable x and Hamiltonian energy H across different f values.

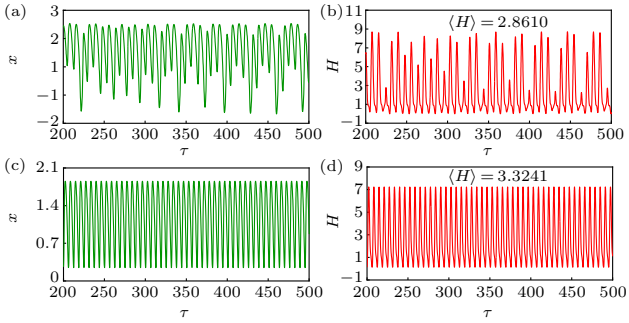


Fig. 5. Evolution of x and H for different f. For (a) and (b) $f=0.79$ (chaotic); (c) and (d) $f=1$ (periodic).

Figure 5 demonstrates that chaotic modes in the multifunctional neural circuit exhibit significantly lower mean Hamiltonian energy $\langle H\rangle$ compared to periodic modes.

Furthermore, we investigate the influence of external electric fields on the circuit dynamics. Maintaining the previous parameters and initial conditions and photic stimulation is set as $u_{\mathrm{s}}=2.75\cos(0.8\tau)$, Fig. 6 presents the BD and LLE for the case where external electrical field intensity S_{ext} equals conductance G.

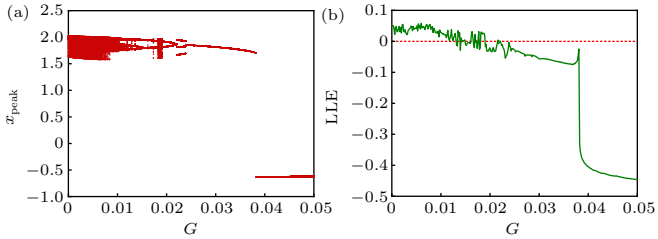


Fig. 6. Evolution of BD and LLE for different G. For (a) BD under $G\in[0,0.05]$; (b) LLE under $G\in[0,0.05]$.

Figure 6 reveals that lower external electric field intensities (S_{ext}) induce chaotic dynamics in the multifunctional neural circuit. As S_{ext} increases, the system undergoes a transition from chaotic to periodic patterns, demonstrating effective chaos suppression through field modulation. Figure 7 further characterizes this transition by showing the corresponding evolution of state variable x and Hamiltonian energy H with varying conductance G.

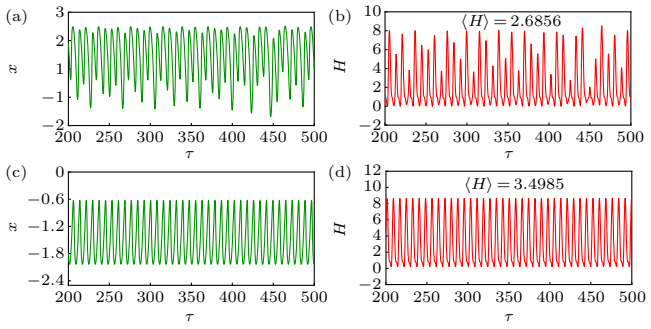


Fig. 7. The x and H by changing G. For (a) and (b) $G = 0.006$ (chaotic); (c) and (d) $G = 0.045$ (periodic).

Similar to the results in Figs. 3 and 5, chaotic patterns in the multifunctional neural circuit exhibit lower mean Hamiltonian energy $\langle H\rangle$, whereas periodic modes show higher $\langle H\rangle$. Figure 8 shows the dynamical response under external electric field stimulation $S_{\text{ext}} = B\cos(0.4\tau)$, consistent with the previous findings. Figure 8 demonstrates that periodic electric field stimulation ($S_{\text{ext}} = B\cos(0.4\tau)$) can induce both chaotic and periodic dynamical modes in the multifunctional neural circuit. Complementing these results, Fig. 9 presents the time evolution of state variables and corresponding Hamiltonian energy under different field amplitudes B.

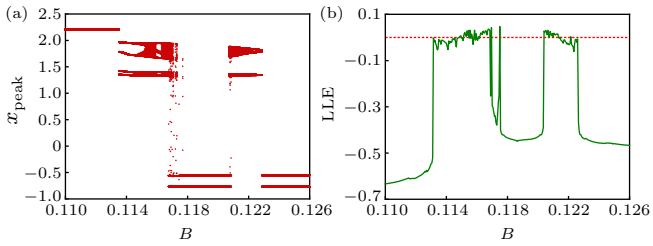


Fig. 8. Evolution of BD and LLE for different B. For (a) BD under $B \in [0.11, 0.126]$; (b) LLE under $B \in [0.11, 0.126]$.

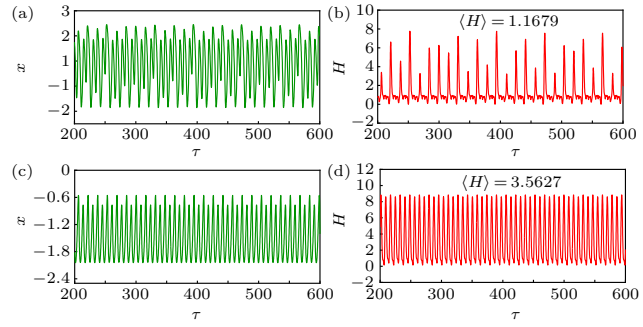


Fig. 9. Evolution of x and H for different B. For (a) and (b) $B = 0.1156$ (chaotic); (c) and (d) $B = 0.124$ (periodic).

Figure 9 demonstrates that chaotic states in the multifunctional neural circuit exhibit significantly lower mean Hamiltonian energy $\langle H\rangle$ compared to periodic states.

In summary, the functional neuron circuits designed using functional electronic components can effectively simulate the electrical activities of real biological neurons. External signals can be effectively detected by functional electronic components. This research provides a theoretical basis for developing intelligence in artificial neural networks.

4. Conclusion

This work presents a novel multifunctional neural circuit comprising two capacitors, two linear resistors, a phototube, a nonlinear resistor, and a charge-controlled memristor. Using Kirchhoff's and Helmholtz's laws, we derived the complete set of circuit equations, dynamic equations, and energy functions of the system. Through comprehensive nonlinear analysis, we demonstrated that the circuit can generate both periodic and chaotic states in response to external light and electric field stimuli. Chaotic states exhibit significantly lower mean Hamiltonian energy $\langle H\rangle$ on average compared to periodic modes. The circuit exhibits high sensitivity to both optical and electrical inputs. The design can be effectively extended to construct functional neural networks for studying coupled neuron dynamics. In future work, we plan to develop additional multifunctional neuron models, implement hardware versions of these models, and explore practical applications of neural networks in engineering.

Acknowledgments

Project supported by the Gansu Provincial Department of Education University Teacher Innovation Fund Project (Grant No. 2024A-168), the Qingyang Science and Technology Plan Project (Grant No. QY-STK-2024B-193), and the Horizontal Research Project of Longdong University (Grant No. HXZK2422).

References

[1] Levi T, Khoyratee F, Saïghi S and Ikeuchi Y 2018 *Artif. Life Robot.* **23** 10
[2] Hayati M, Nouri M and Haghiri S 2015 *IEEE Trans. Circuits Syst. I* **62** 1805
[3] Brette R and Gerstner W 2005 *J. Neurophysiol.* **94** 3637
[4] Hindmarsh J L and Rose R M 1982 *Nature* **296** 162
[5] Chay T R 1985 *Physica D* **16** 233
[6] Izhikevich E M 2003 *IEEE Trans. Neural Netw.* **14** 1569
[7] Muni S S, Fatoyinbo H O and Ghosh I 2022 *Int. J. Bifurcation Chaos* **32** 2230020
[8] Liu Y, Xu W, Ma J, Alzahrani F and Hobiny A 2020 *Front. Inf. Technol. Electron. Eng.* **21** 1387
[9] Xu Y, Guo Y, Ren G and Ma J 2020 *Appl. Math. Comput.* **385** 125427
[10] Guo Y, Zhou P, Yao Z and Ma J 2021 *Nonlinear Dyn.* **105** 3603
[11] Song X and Yang F 2024 *Phys. Scr.* **99** 125247
[12] Yang F, Guo Q, Ren G and Ma J 2024 *J. Biol. Phys.* **50** 271
[13] Xu Y, Liu M, Zhu Z and Ma J 2020 *Chin. Phys. B* **29** 098704
[14] Xie Y, Ye Z, Li X, Wang X and Jia Y 2024 *Cogn. Neurodyn.* **18** 1989

[15] Yang F, Han Z, Ren G, Guo Q and Ma J 2024 *Eur. Phys. J. Plus* **139** 534
[16] Wu F, Hu X and Ma J 2022 *Appl. Math. Comput.* **432** 127366
[17] Yang F, Xu Y and Ma J 2023 *Chaos* **33** 023110
[18] Yang F, Ren G and Tang J 2023 *Nonlinear Dyn.* **111** 21917
[19] Song X and Yang F 2025 *J. Theor. Biol.* **599** 112034
[20] Guo Y, Wu F, Yang F and Ma J 2023 *Chaos* **33** 113106
[21] Yang F, Song X and Yu Z 2024 *Chaos Solitons Fractals* **188** 115496
[22] Wan J, Wu F, Ma J and Wang W 2024 *Chin. Phys. B* **33** 050504
[23] Yang F, Song X and Yu Z 2025 *Nonlinear Dyn.* **113** 7213
[24] Yu Z, Zhu K, Wang Y and Yang F 2025 *Chaos Solitons Fractals* **194** 116233
[25] Yang F, Song X and Xu Y 2025 *Chaos Solitons Fractals* **199** 116740
[26] Mao Y, Dong Y, Lu Z, Xiang C, Wang J and Liang Y 2025 *Chaos Solitons Fractals* **195** 116279
[27] Xu Q, Wang Y, Iu H H C, Wang N and Bao H 2023 *IEEE Trans. Circuits Syst. I* **70** 3130
[28] Lin H, Wang C, Sun Y and Yao W 2020 *Nonlinear Dyn.* **100** 3667
[29] Park H, Han J K, Yim S, Shin D H, Park T W, Woo K S, Lee S H, Cho J M, Kim H W, Park T and Hwang C S 2025 *Adv. Mater.* **37** 2412549
[30] Chen Y, Lai Q, Zhang Y, Erkan U and Toktas A 2024 *Nonlinear Dyn.* **112** 8603
[31] Zhou L, Lin H and Tan F 2024 *Neurocomputing* **577** 127384
[32] Bao B, Hu J, Cai J, Zhang X and Bao H 2023 *Nonlinear Dyn.* **111** 3765
[33] Liu B, Peng X and Li C 2024 *AEU-Int. J. Electron. Commun.* **178** 155283
[34] Ma T, Mou J and Chen W 2025 *Chaos Solitons Fractals* **198** 116537
[35] Cao H, Wang Y, Banerjee S, Cao Y and Mou J 2024 *Chaos Solitons Fractals* **179** 114466
[36] Ramakrishnan B, Mehrabbeik M, Parastesh F, Rajagopal K and Jafari S 2022 *Electronics* **11** 153